

# Dust Grain Damage to Interstellar Laser-Pushed Lightsail

James T. Early\* and Richard A. London†

*Lawrence Livermore National Laboratory, Livermore, California 94550*

Lightsails pushed by laser beams to velocities around  $0.1c$  have been proposed as propulsion systems for interstellar travel. These lightsails will undergo high-energy collisions with small ( $\sim 1\text{-}\theta$  m) dust grains in the interstellar environment. For a very thin beryllium sail, the grains pass through the sail with only  $10^{-4}$  of the energy coupled into the sail. The resulting damaged area is not significantly larger than the cross section of the dust grain. Only a small fraction ( $10^{-6}$ – $10^{-4}$ ) of the sail will be destroyed by these  $1\text{-}\theta$  m-sized grains during the sail acceleration. For thick sails or larger grains, the damage can be more significant.

## Nomenclature

$A$	= atomic number
$a_o$	= Bohr radius, $0.53 \times 10^{-8}$ cm
$b$	= impact parameter, cm
$c$	= speed of light
$c_s$	= ion-acoustic velocity, cm/s
$D_e$	= electron thermal diffusivity, $\text{cm}^2/\text{s}$
$E$	= ion or electron energy, eV
$E_V$	= energy/volume, $\text{erg}/\text{cm}^3$
$e$	= charge of electron, $1.6 \times 10^{-19}$ C
$F$	= radiation flux, $\text{erg}/\text{cm}^2$ s
$k$	= Boltzmann's constant, $1.380 \times 10^{-16}$ erg/K
$L$	= luminosity, erg/s
$M$	= total mass, g
$m$	= mass per particle, g
$m_o$	= $1.67 \times 10^{-24}$ g
$N$	= total number of ions or electrons
$n$	= number density, number/ $\text{cm}^3$
$R$	= distance from grain to foil surface, cm
$r$	= radius, cm
$T$	= temperature, eV
$t$	= time, s
$u$	= ratio of particle velocity to electron thermal velocity, $v/v_{te}$
$V$	= volume, $\text{cm}^3$
$v$	= velocity, cm/s
$x$	= distance, cm
$Z$	= number of electrons per atom
$\alpha$	= fine structure constant, $\frac{1}{137}$
$\beta$	= velocity ratio, $v/c$
$\gamma$	= $1/[1 - (v/c)^2]^{1/2}$
$\Delta x$	= thickness, cm
$\epsilon_b$	= bremsstrahlung emissivity, $\text{erg}/\text{cm}^3$ s
$\epsilon_o$	= $8.85 \times 10^{-12}$ C/Vm
$\Lambda$	= impact parameter ratio
$\lambda_D$	= debye length, cm
$\rho$	= mass density, $\text{g}/\text{cm}^3$
$\sigma$	= cross section, $\text{cm}^2$

## Subscripts

$b$	= bremsstrahlung
$c$	= collision
$e$	= electron
$f$	= foil
$g$	= grain
$h$	= hydrodynamic

$i$	= ion
$o$	= original value
$p$	= particle
$t$	= target

## Introduction

FOR travel to nearby stars, velocities around  $0.1c$  will be the minimum required for missions of the order of a human lifetime. Higher velocities and shorter mission times can be achieved only at horrendous costs in energy. There are relatively few technical concepts that hold out the possibility of accomplishing this objective, and all of the options have extraordinary technical challenges and expected expense.

One option is to use the momentum transfer from reflecting laser photons off a very light weight sail to propel a vehicle. This concept<sup>1,2</sup> requires large space-based optics, laser powers, and sail designs that are all far beyond today's technology but that are conceivable. For this concept the laser light absorbed by the sail will result in a thermal limit on the maximum possible laser power densities and, as a result, a maximum acceleration. The resulting low acceleration then requires distances up to 0.1 light year to achieve the cruise velocity. The lightsail does not need to be deployed during the cruise phase of the voyage, but it must be deployed again if the lightsail is also used to decelerate at the target star.<sup>2</sup>

The laser sail will interact with the local interstellar environment during these acceleration periods. The large velocity difference between the sail and local dust particles results in the potential release of significant energies during these collisions.<sup>3</sup> If much of this energy were coupled into the sail, there could be significant damage.

In this paper we will first specify typical mission parameters. The collision mechanisms will be analyzed to determine the energy released by collisions. Finally, the impact on the lightsails of this energy release will be discussed.

## Local Interstellar Environment

Local interstellar dust properties can be estimated from dust impact rates on spacecraft in the outer solar system and by dust interaction with starlight. The mean particle masses seen by the Galileo and Ulysses spacecraft were  $2 \times 10^{-12}$  and  $1 \times 10^{-12}$  g, respectively. A  $10^{-12}$ -g dust grain has a diameter of approximately  $1 \mu\text{m}$ . The median grain size is smaller because the mean is dominated by larger grains. The Ulysses saw a mass density of  $7.5 \times 10^{-27}$  g  $\cdot$  cm $^{-3}$  or a mean particle number density of  $7.5 \times 10^{-15}$  cm $^{-3}$ . A sail accelerating over a distance of 0.1 light years would encounter 700 dust grains/cm $^2$  at this density.

Note that neither Voyager spacecraft saw any dust grains larger than  $1 \mu\text{m}$  at distances beyond 50 astronomical units. A report by Frisch et al.<sup>4</sup> on the state of knowledge of interstellar dust grain distributions shows a flat distribution from  $10^{-14}$  to  $10^{-12}$  g, with some grains as large as  $10^{-11}$  g.

For this report a  $1\text{-}\mu\text{m}$ -diam grain will be used for impact calculations.

Received 3 May 1999; revision received 10 February 2000; accepted for publication 16 March 2000. Copyright © 2000 by the American Institute of Aeronautics and Astronautics, Inc. All rights reserved.

\*Deputy Program Leader, Laser Directorate, P.O. Box 808. Member AIAA.

†Group Leader, X Division, P.O. Box 808.

### Typical Laser Sail Properties

Laser sail performance is driven by the ratio of the thermally limited laser power density divided by the mass per unit area. Reviews of possible laser sail materials by Landis<sup>5,6</sup> show three general sail types. First are the very thin ( $\sim 20$  nm), low-density metal sails such as the aluminum sail proposed by Forward.<sup>2</sup> Beryllium appears to be the best material in this category. Very thin refractory metals such as niobium or tantalum, which could operate at higher temperatures and power densities, are a second option. Dielectric thin films at one-quarter wavelength thickness for the laser light have good optical reflectivity. The dielectric materials require thicker sails, but their low absorption and refractory behavior give good thermal performance and result in potentially better accelerations. In addition, carbon sails suggested by Forward have low reflectivity but can operate at a very high temperature.

The thin beryllium sail is currently the best characterized design, and it will be used as a reference case. The sail is assumed to be 20 nm thick, and the normal bulk properties of beryllium are used.

### Electron Heating During Collisions

Collisions between nuclei will be ignored in this problem due to the low probability of such events. If we assume a 10 barn cross section for such momentum scattering collisions, then the probability of large angle scattering is very small:

$$n\sigma\Delta x \sim (5 \times 10^{22}/\text{cm}^2)(10^{-23} \text{ cm}^2)(10^{-4} \text{ cm})(\Delta x/1 \mu\text{m}) \\ = 5 \times 10^{-5}(\Delta x/1 \mu\text{m})$$

The main coupling of translational energy between the foil and grain will be due to ion–electron collisions. The grain and foil atoms are stripped of bound electrons early in the collision. The energy loss rate for high-energy collisions between ions and free electrons can be calculated using the simplifying assumption that the fractional energy loss per collision is small, and, thus, the particle paths are approximately straight during the collision. The electron is then given a small net impulse in the direction perpendicular to the line of flight of the ion. Because we are interested in the heating of both the foil and the grain, we consider ions in a particle and electrons in a target. The particle and target can be the grain and foil or vice versa. From Refs. 7 and 8 the ion energy loss  $dE$  while passing a distance  $dx$  through a target material is then

$$\left(\frac{dE}{dx}\right)_{pi} = \frac{4\pi e^4 Z_p^2 n_t Z_i}{m_e v^2} G(u) \cdot \ell_n \Lambda \quad (1)$$

where

$$n_t = \rho_t / A_t m_t, \quad v_{te} = (2kT_e / m_e)^{1/2}, \quad \Lambda = b_{\max} / b_{\min}$$

$b_{\max} / b_{\min}$  is the maximum impact parameter/minimum impact parameter and  $G(u)$  is a factor accounting for the electron velocity in target<sup>7</sup>:

$$G(u) = \text{erf}(u) - u \text{erf}'(u) \sim \frac{3}{4}u^3$$

for  $u \ll 1$ , where the coulomb logarithm term ( $\ell_n \Lambda$ ) is usually determined by an ionization limit or by electron debye shielding; in this case we must consider the ion sphere cutoff due to the high density of ions in the particle. The maximum impact parameter is, therefore,

$$b_{\max} = r_{\text{ion}} = (4\pi n_p / 3)^{-1/3}$$

where  $r_{\text{ion}}$  is the ion sphere radius of particle and the density of particle atoms is used because ions would shield each other for larger  $b$ .

The minimum impact parameter is set to the radius at which the coulombic potential energy is equal to the kinetic energy and where large angle electron scattering would occur<sup>8</sup>:

$$b_{\min} = Z_p e^2 / \gamma m_e v^2$$

Therefore, we have

$$\Lambda = \frac{r_{\text{ion}}}{b_{\min}} = \frac{\gamma m_e v^2 (n_p / 4\pi / 3)^{-1/3}}{Z_p e^2} = \frac{\gamma \beta^2}{Z_p \alpha^2} \left(\frac{r_i}{a_o}\right) \quad (2)$$

The resulting heating of target can be calculated from the energy loss:

$$\Delta E_{et} = \left(\frac{dE}{dx}\right)_{pi} \cdot \frac{\Delta x_t N_{ip}}{N_{et}} \quad (3)$$

which is equal to the energy change per target electron. Similarly, to find the velocity change of target, we use momentum conservation:

$$\Delta v_t = \Delta v_p M_p / M_t \\ N_{et} \Delta E_{et} = \frac{1}{2} M_p \Delta(v_p^2) \sim M_p v \Delta v_p \quad \text{for} \quad (\Delta v_p \ll v) \\ \Delta v_t = N_{et} \Delta E_{et} / M_t v \quad (4)$$

and substitute into Eq. (4) for the foil,

$$\Delta v_f = \left(\frac{dE}{dx}\right)_{gi} \cdot \frac{4}{3} \cdot r_g \frac{\rho_g / \rho_f}{m_{gi} v} \quad (5)$$

Put constants into Eq. (1):

$$\left(\frac{dE}{dx}\right)_{pi} = 306 \frac{\text{keV}}{\text{cm}} Z_p^2 Z_t \left(\frac{\rho_t}{A_t}\right) \beta^{-2} G(u) \ell_n \Lambda \quad (6)$$

This formula may be applied to either the foil or the grain as the target, with the other as the particle. The electron–electron collisions that have been ignored do not contribute as much to the heating due to their lower charge relative to the nucleus, that is,  $Z_p = 1$  for electrons.

### Results for a Typical Example

As an example we assume a 20-nm beryllium foil that is traveling at  $0.1c$  and that collides with a  $1\text{-}\mu\text{m}$ -diam dust grain. We will assume silicon as typical of dust grain atoms. The following parameter values are assumed:  $Z_f = 4$ ,  $A_f = 9$ ,  $\rho_f = 1.85 \text{ g/cm}^3$ ,  $n_f = 1.23 \times 10^{23} \text{ cm}^{-3}$ ,  $Z_g = 14$ ,  $A_g = 28$ ,  $\rho_g = 2.3 \text{ g/cm}^3$ ,  $n_g = 4.97 \times 10^{22} \text{ cm}^{-3}$ ,  $\Delta x_f \sim 20 \text{ nm} = 2 \times 10^{-6} \text{ cm}$ ,  $r_g = 0.5 \mu\text{m} = 0.5 \times 10^{-4} \text{ cm}$ ,  $r_{ig} = 1.7 \times 10^{-8} \text{ cm}$ ,  $r_{if} = 1.25 \times 10^{-8} \text{ cm}$ , and  $v = 0.1c$ .

First consider heating of the foil. The beryllium foil is the target, and the silicon grain atoms are the particles. Equation (2) for  $\Lambda$  becomes

$$\Lambda = (\gamma \beta^2)^{1/2} \alpha^2 Z_g (r_{ig} / a_o) = 43(\beta / 0.1)^2 (Z_g / 14)^{-1} (r_{ig} / 1.7 \text{ \AA})$$

By the use of  $\Lambda$ , Eq. (6) for the 131-MeV silicon ion becomes

$$\left(\frac{dE}{dx}\right)_{gi} = 1.85 \frac{\text{MeV}}{\mu\text{m}} \left(\frac{Z_g}{14}\right)^2 \left(\frac{Z_f}{4}\right) \left(\frac{n_f}{1.23 \times 10^{23}}\right) \left(\frac{\beta}{0.1}\right)^{-2} \\ \times \left(\frac{\ell_n \Lambda}{3.76}\right) G(u)$$

Then the heating of foil is from Eq. (3):

$$\Delta E_{ef} = \left(\frac{dE}{dx}\right)_{gi} \Delta x_f \cdot \frac{N_{ig}}{N_{ef}} = \frac{n_{ig}}{n_{ef}} \left(\frac{dE}{dx}\right)_{gi} \cdot \frac{4}{3} r_g \\ = \frac{\rho_g / A_g}{\rho_f Z_f / A_f} \cdot \int_0^{4r_g/3} \left(\frac{dE}{dx}\right)_{gi} dx = 0.10 \int_0^{4r_g/3} \left(\frac{dE}{dx}\right)_{gi} dx$$

for  $r_g = 0.5 \mu\text{m}$ ,

$$\Delta E_{ef} = 185 \text{ keV} \int_0^{2\mu\text{m}} G(u) dx \quad (7)$$

The heating of the foil electrons to energies where their thermal velocity is greater than  $v$ , that is,  $u < 1$ , results in lower heating rates as reflected in the lower values of  $G(u)$ . Numerical integration of Eq. (7) yields  $\Delta E_{ef} \sim 21$  keV and  $T_{ef} = \frac{2}{3} \Delta E_{ef} \sim 14$  keV. Also from Eq. (5),  $\Delta v_f = 3 \times 10^6$  cm/s  $= 0.001v$ .

Next, consider heating of the grain. The grain electrons are the targets, and the beryllium atoms are the particles. By using the same numerical example, the coulomb term becomes  $\Lambda = 110$ , and the beryllium particle energy loss from Eq. (6) is

$$\left( \frac{dE}{dx} \right)_{fi} = 265 \frac{\text{keV}}{\mu\text{m}} G(u) \quad (8)$$

The grain electron velocities remain below the collision velocity, so that  $u$  is greater than 1 and  $G \sim 1$ :

$$\begin{aligned} \Delta E_{eg} &= \left( \frac{dE}{dx} \right)_{fi} \frac{4}{3} \cdot r_g \cdot \frac{N_{if}}{N_{eg}} \\ \Delta E_{eg} &= \left( \frac{dE}{dx} \right)_{fi} \cdot n_{if} \frac{\Delta x_f}{n_{eg}} = \left( \frac{dE}{dx} \right)_{fi} \cdot \frac{\rho_f / A_f}{Z_g \rho_g / A_g} \Delta x_f \\ &= 0.179 \cdot \left( \frac{dE}{dx} \right)_{fi} \cdot \Delta x_f \end{aligned} \quad (9)$$

Equations (8) and (9) then yield  $\Delta E_{eg} = 0.95$  keV and  $T_{eg} = 0.63$  keV.

The electron heating can be evaluated for a range of collision velocities for this example. The results are shown in Figs. 1 and 2 for the grain electrons and Figs. 3 and 4 for the foil electrons. Figures 1–4 do not extend below velocities of  $0.02c$  because the high collision energy assumptions in Eq. (2) are not valid for lower velocities.

In these calculations we have ignored the possibility of electron exchange between foil and grain electrons. As long as the grain electron thermal velocity is less than the collision velocity ( $u > 1$  in Fig. 1), electron exchange would require a significant acceleration

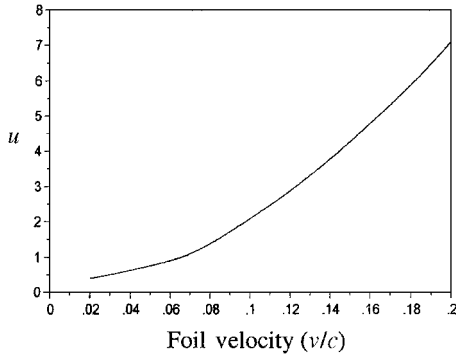


Fig. 1 Velocity ratio  $u$  (foil velocity/electron velocity) for grain electrons.

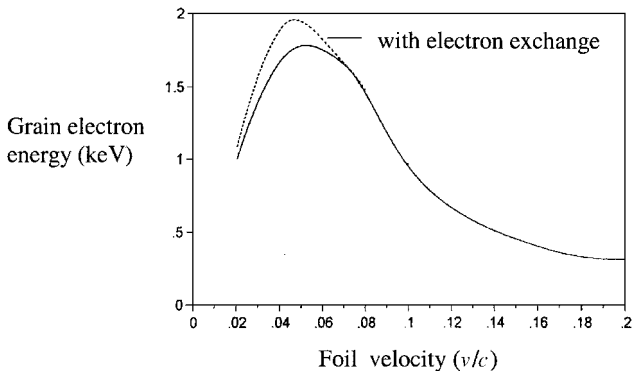


Fig. 2 Grain electron energy.

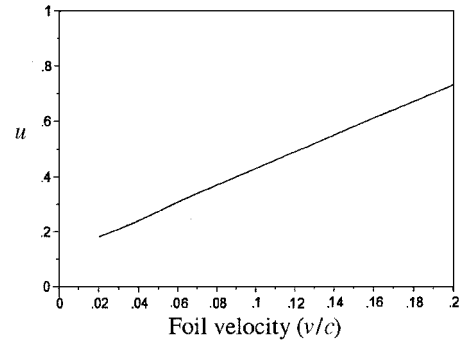


Fig. 3 Velocity ratio  $u$  (foil velocity/electron velocity) for foil electrons.

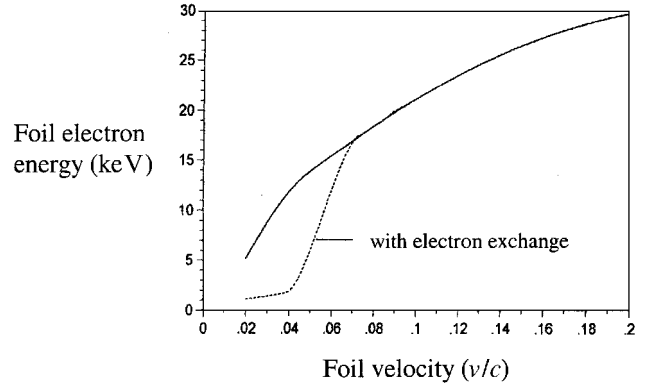


Fig. 4 Foil electron energy.

of the grain electrons, and the no-exchange approximation appears reasonable. For collision velocities below  $0.07c$ , the grain electrons have adequate thermal velocities to exchange with the hotter foil electrons. Because the number of grain electrons is much larger than the number of foil electrons, the additional energy supplied to the grain electrons by electron exchange is relatively small, as can be seen in Fig. 2. By contrast this exchange mechanism will have a strong impact on the foil electron energy at low collision velocities. The foil electron energy is effectively clamped at the grain electron energy because the electrons now move freely between the two populations. The impact is illustrated in Fig. 4 by plotting the average electron energy for  $v < 0.07c$ . To more accurately calculate the foil electron heating at low velocities requires a complicated, coupled solution.

### Explosion of the Heated Foil

In the region where the dust grain passed, the foil electrons are left at very high temperatures. The high energy of the foil electrons will take them beyond the surface of the foil. The lowered electron density in the foil will give a surface charge density that sets up an electric field to retain the electrons, that is, an ambipolar diffusion field. This field then accelerates the ions to high velocities and converts the electron energy into ion kinetic energy. The high aspect ratio of this geometry should make this a primarily one-dimensional expansion.

References 9 and 10 give a detail analysis of a one-dimensional plasma expansion into a vacuum. A simplified self-similar solution to the ion equations of motion gives

$$v_i = c_s + x/t, \quad n_i = n_0 \exp[-(1 + x/c_s t)]$$

The expansion wave propagates into the foil at the ion-acoustic velocity  $c_s$  giving the linear ion velocity and exponential density profile (Figs. 5 and 6). A more complete description of the expansion may be found in the references, but the simple self-similar solution will suffice for this paper. When both expansion waves reach the opposite sides of the foil, most  $(2/e)$  of the foil ions have expanded beyond the original boundaries. After this time the reflected

expansion waves create a more complex solution. We will define this as the foil hydrodynamic time  $t_{hf}$ :

$$c_{sf} = (z_f k T_e / m_i)^{1/2} \sim 7.72 \times 10^7 \text{ cm/s}$$

$$t_{hf} = \Delta x_f / c_{sf} \sim 2.6 \times 10^{-14} \text{ s} = 26 \text{ fs}$$

The time required to heat the ions by collisions with the electrons is orders of magnitude longer than the time required to accelerate the ions with these electron generated electric fields. Thus, the energy of the hot electrons is almost totally converted into the kinetic energy of this one-dimensional expansion of the ions. This expansion should result in negligible damage to the remainder of the foil outside of the area contacted by the dust grain. We shall next consider two mechanisms that could couple the collision energy into the remainder of the foil.

### Electron Thermal Diffusion During Foil Explosion

While the expansion of the heated foil is occurring, the hot electrons can also heat the adjacent foil area by thermal diffusion. The electron thermal diffusivity  $D_e$  is<sup>11</sup>

$$D_e \sim v_e / n_{if} (4\pi b^2) \ln(\lambda_D / b) \propto T_e^{2.5}$$

where  $b$  is the minimum impact parameter equal to  $z_f e^2 / (4\pi \epsilon_0) 3kT_{ef}$  and  $\lambda_D$  is Debye length equal to  $[\epsilon_0 k T_e / e^2 n_e]^{1/2}$ . For  $T_e \sim 10 \text{ keV}$ ,  $D_e \sim 10^5 \text{ cm}^2/\text{s} = 0.1 \mu\text{m}^2/\text{fs}$ .

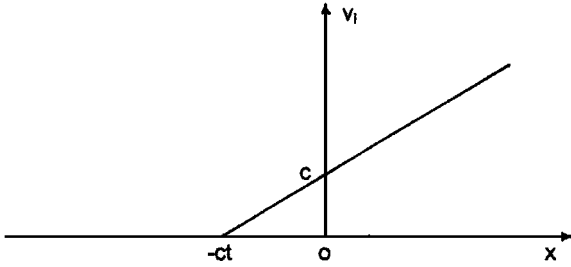


Fig. 5 Linearly increasing ion velocity  $v_i$ .

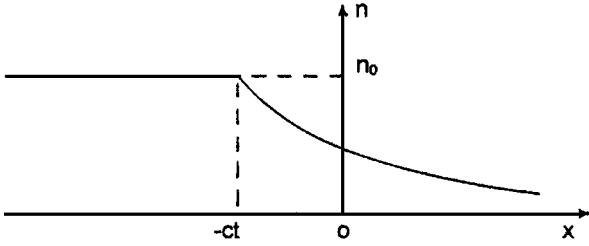


Fig. 6 Plasma expansion generates exponential density profile.

Because the electron diffusivity has a strong temperature dependence, the thermal diffusion equation must be solved numerically (Fig. 7). The high thermal diffusivity in the heated region flattens the central temperature profile. The temperature dependence also causes the sharp temperature profile near the edge. The impact of thermal diffusion does not lead to a substantial increase in the foil damage area.

### Bremsstrahlung Radiation Effects

The high-energy free electrons will generate significant bremsstrahlung radiation during their interaction with the ions. This radiation will not significantly cool the foil before it explodes. The grain, however, will take longer to explode, and the radiation from the grain could continue to heat the foil outside the collision region after the collision.

The emissivity of bremsstrahlung radiation from a hot, optically thin plasma<sup>12</sup> is

$$\epsilon_b = 1.4 \times 10^{-27} T_e^{1/2} n_e n_i Z_i^2 \text{ (erg/cm}^3 \text{ s)}$$

where  $n$  is in  $\text{cm}^{-3}$  and  $T_e$  in Kelvin. The electron cooling time  $t_b$  is then

$$t_b = 3n_e k T_e / 2\epsilon_b = 1.5k T_e^{1/2} / 1.4 \times 10^{-27} n_i Z_i^2 \text{ s}$$

$$= (8.43 \times 10^{-10} \text{ s}) \cdot T_{\text{keV}}^{1/2} (n_i / n_o)^{-1} Z_i^{-2}$$

For the foil,  $n_i \sim 1.23 \times 10^{23}$ ,  $Z_i = 4$ ,  $T_e = 14 \text{ keV}$ , and

$$t_{bf} \sim 0.96 \times 10^{-9} \text{ s}$$

For the grain,  $n_i \sim 0.49 \times 10^{23}$ ,  $Z_i = 14$ ,  $T_e = 0.63 \text{ keV}$ , and

$$t_{bg} \sim 42.0 \times 10^{-12} \text{ s}$$

The collision duration is short compared to these cooling times:

$$t_c = 2r_g / V = 10^{-4} / 3 \times 10^9 = 0.3 \times 10^{-13} \text{ s} = 33 \text{ fs}$$

If, like for the foil, we define a characteristic hydrodynamic flow time for the grain  $t_h$

$$t_{hg} = r_g / c_{sg} \sim 2.9 \times 10^{-12} \text{ s} = 2.9 \text{ ps}$$

where  $c_{sg} \sim 1.7 \times 10^7 \text{ cm/s}$ , then the radiation efficiency is  $\sim t_h / t_b \sim 2.7 \times 10^{-5}$  for the foil and  $\sim 0.069$  for the grain.

The foil energy will be converted to kinetic energy before radiative cooling plays a significant role. Most of the grain energy will also go into kinetic energy. Because the grain velocity is much larger than the resulting ion velocities  $\sim c_s$ , the grain ions will not collide with the foil. The radiation from the grain, however, could heat the foil.

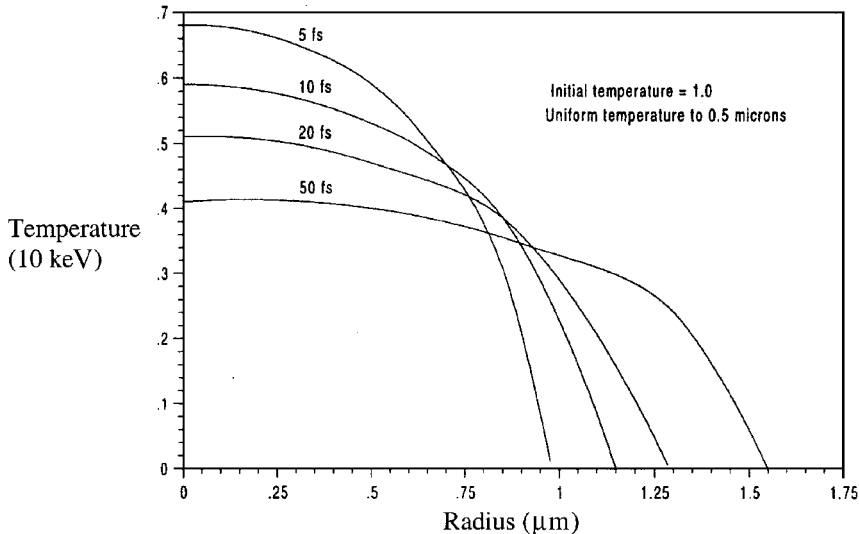


Fig. 7 Temperature distributions with electron thermal diffusion after collision.

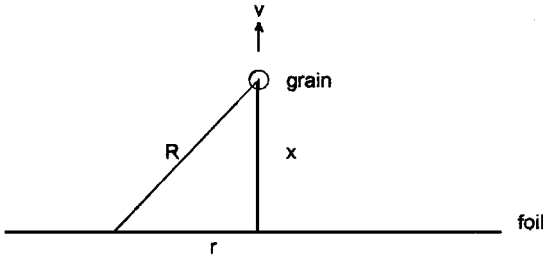


Fig. 8 Geometry after collision.

If we compare the total energy in grain and foil using

$$E_{\text{tot}} = \Delta E_e \cdot N_e$$

we find

$$E_{\text{tot } f} = 21. \text{ keV} \cdot \pi r_g^2 n_{ef} \Delta x_f$$

$$E_{\text{tot } g} = 0.95 \text{ keV } 4\pi r_g^3 \cdot 3 \cdot n_{eg}$$

The ratio is

$$\frac{E_{\text{tot } g}}{E_{\text{tot } f}} = 0.045 \cdot \frac{4r_g n_{eg}}{3n_{ef} \Delta x_f} \sim 1.51 \frac{Z_g \rho_g / A_g}{Z_f \rho_f / A_f} \sim 2.1$$

Because the grain may have similar energy to the foil and radiates that energy efficiently, the reradiation of grain energy could be important if it couples into the foil. For radiation at  $\frac{1}{2}$  keV the optical depth  $\tau$  of cold Be is small for the thin foil:

$$\tau = \rho \kappa \Delta x \sim 0.0185$$

where  $\kappa$  is the opacity equal to  $5 \times 10^3 \text{ cm}^2/\text{g}$  (Ref. 13).

To calculate the recoupling of grain radiation to the foil after a collision, we must calculate the rate of energy absorption as the particle moves away from the foil (Fig. 8). The heating rate of the foil is

$$\frac{dE_V}{dt} = F \cdot \rho \kappa$$

where  $E_V$  is the energy/volume and  $F$  is the flux of radiation from grain to foil,

$$F = L/4\pi R^2$$

where  $L$  is grain luminosity, and  $R$  is the distance from the grain to a position  $r$  on the foil surface,  $R^2 = x^2 + r^2 = r^2 + v^2 t^2$ .

The internal energy increase of the foil is

$$\begin{aligned} \Delta E &= \int F \rho \kappa dt = \frac{\rho \kappa L}{4\pi} \int_{r_g}^{r_{hg}} \frac{dt}{r^2 + v^2 t^2} \\ &= \left( \frac{\rho \kappa L}{4\pi} \right) \left( \frac{1}{rv} \right) \cdot \tan^{-1} \left( \frac{vt_{hg}}{r} \right) \end{aligned}$$

where for the grain,

$$\frac{vt_{hg}}{r} = \frac{vr_g}{c_{sg} r} \sim \frac{3 \times 10^9}{1.7 \times 10^7} \cdot \frac{r_g}{r} \sim 176 \frac{r_g}{r}$$

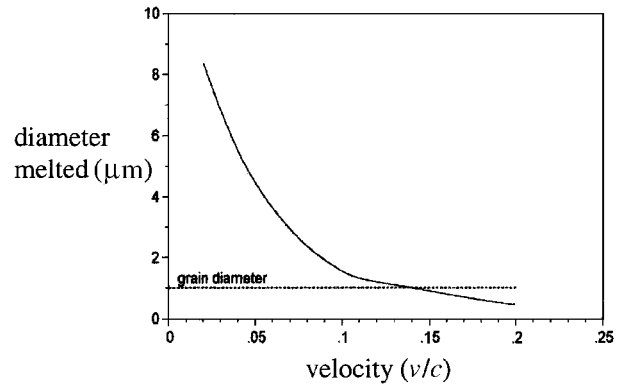
for  $r \ll 176 r_g$ ,  $\tan^{-1}(vt_{hg}/r) \sim \pi/2$ , and  $\Delta E_V = \rho \kappa L/8rv$ .

Defining  $V_g$  as the volume equal to  $4\pi r_g^3/3 = 0.52 \times 10^{-12} \text{ cm}^3$ , we find

$$L = \varepsilon_b \cdot V_g = (2.52 \times 10^{25} \text{ erg/cm}^3 \text{ s}) \cdot V_g = 1.31 \times 10^{13} \text{ erg/s}$$

This gives

$$\Delta E_V \sim 5.06 \times 10^{10} (r/1 \mu\text{m})^{-1} \text{ erg/cm}^3$$

Fig. 9 Diameter of hole melted in foil by radiation from 1- $\mu\text{m}$  grain.

Using  $\rho C_p \sim 3n_{if}k = 5.1 \times 10^7 \text{ erg/cm}^3/\text{K}$ , we find

$$\Delta T = \Delta E_V / \rho C_p \sim 992 \text{ K} (r/1 \mu\text{m})^{-1}$$

where  $r/1 \mu\text{m} \sim 992 \text{ K} / \Delta T$ .

Because the melting temperature for Be is 1278 K, the radiative heating from a 1- $\mu\text{m}$ -diam particle will not be an issue much beyond the area already heated by the grain passage.

The scaling of the region of the foil melted by thermal radiation from the grain is

$$r \propto (r_g^3 Z_g^3 n_{ig}^2) v^{-2} \left( \frac{Z_f^2}{\Delta T_{\text{melting}}} \right) \left[ n_{if} \int^{\Delta x_f} G(u) dx \right]^{\frac{1}{2}} \quad (10)$$

Because the radiative heating from the grain is proportional to the grain volume  $r_g^3$ , for larger grains the radiative heating would melt areas larger than the grain cross section. The values of  $n$  and  $z$  for the grains should be close to the values used in this example. The velocity dependence results in more radiation damage in low-velocity collisions. The  $G(u)$  term lowers the grain electron temperature and the resulting damage. Figure 9 shows the damage from a 1- $\mu\text{m}$  grain.

### Summary

The scaling of the melting due to thermal radiation [Eq. (10)] may influence the design of laser sails. There have been three generic types of laser sails considered. For the ultrathin, moderate melting point metal shield, beryllium appears to be the best material because of its low atomic mass and its high melting point. Increasing the beryllium sail thickness, if necessary, will not rapidly increase the damaged area. The second sail type was ultrathin refractory metal foils such as tantalum that could operate at higher temperatures and higher laser power densities. It can be seen that the higher atomic mass would result in more damage to such sails. The damage will be tempered by the  $G(u)$  term, which lowers the particle energy loss rate when the grain electron velocities approach and exceed  $v$ . In general the level of damage to thin laser lightsails appears to be quite small; therefore, the design of these sails should not be strongly influenced by dust collision concerns.

The final sail type is thicker ( $\sim 1 \mu\text{m}$ ) and is made with one or more optical layers of refractory oxides to achieve very low absorptivity. This type of foil would also suffer more thermal radiation damage from heated dust grains due to the greater thickness and molecular weights. The more important damage mechanism for these thicker sails would be the blast damage caused by the explosion of the heated foil section. With the foil depth comparable to the diameter of the heated section, the explosion of this section will no longer have the primarily two-dimensional character of the thin foil. The resulting three-dimensional explosion will couple more kinetic energy into the adjacent foil area. A more complete analysis of the blast wave dynamics will be required for these thicker sails.

### References

- Forward, R. L., "Pluto—The Gateway to the Stars," *Missiles and Rockets*, Vol. 10, April 1962, pp. 26–28.

<sup>2</sup>Forward, R. L., "Round-Trip Interstellar Travel Using Laser-Pushed Lightsails," *Journal of Spacecraft and Rockets*, Vol. 21, No. 2, 1984, pp. 187–195.

<sup>3</sup>Forward, R. L., "Correspondence," *Journal of the British Interplanetary Society*, Vol. 39, No. 7, 1986, p. 328.

<sup>4</sup>Frisch, P. C., Dorschner, J. M., Geiss, J., Greenberg, J. M., Grün, E., Landgraf, M., Hoppe, P., Jones, A. P., Krätschmer, W., Linde, T. J., Morfill, G. E., Reach, W., Slavin, J. D., Svestka, J., Witt, A. N., and Zank, G. P., "Dust in the Local Interstellar Wind," *Astrophysical Journal*, Vol. 525, No. 1, 1999, pp. 492–516.

<sup>5</sup>Landis, G. A., "Small Laser-Pushed Lightsail Interstellar Probe: A Study of Parameter Variation," *Journal of the British Interplanetary Society*, Vol. 50, 1997, pp. 149–154.

<sup>6</sup>Landis, G. A., "Optics and Materials Considerations for a Laser-Propelled Lightsail," International Astronautical Federation, Paper 89-664, Oct. 1989.

<sup>7</sup>Spitzer, L., *Physics of Fully Ionized Gases*, Wiley, New York, 1962, Chap. 5.

<sup>8</sup>Jackson, J., *Classical Electrodynamics*, Wiley, New York, 1967, Chap. 13.

<sup>9</sup>Denavit, J., "Collisionless Plasma Expansion into a Vacuum," *Physics of Fluids*, Vol. 22, No. 7, 1979, p. 1384.

<sup>10</sup>Mora, P., and Pellat, R., "Self-Similar Expansion of a Plasma into a Vacuum," *Physics of Fluids*, Vol. 22, No. 12, 1979, p. 2300.

<sup>11</sup>Mitchner, M., and Kruger, C., *Partially Ionized Gases*, Wiley, New York, 1973, pp. 57, 94.

<sup>12</sup>Osterbrock, D., *Astrophysics of Gaseous Nebulae*, Freeman, San Francisco, 1974, p. 44.

<sup>13</sup>Henke, B. L., Gullikson, E. M., and Davis, J. C., *Atomic and Nuclear Data Tables*, Vol. 54, 1993, pp. 181–342.

A. C. Tribble  
Associate Editor